Supporting information

Synergistic effect of Co^{II}, Ni^{II} and Fe^{II}/Fe^{III} in trimetallic MOFs for enhancing electrocatalytic water oxidation

Yaling Wu,[†] Zhaopeng Sun,[†] Lingmeng Yu,[†] Yingying Chen,[†] Zhibo Li,[†] Mengli Li,[†] Dan Liu,[†] Zheng Yan,[*†] and Xuebo Cao[*,†]

[†] College of Biological, Chemical Sciences and Engineering, Jiaxing University, Jiaxing 314001, P. R. China

* Correspondence to: yzheng158@zjxu.edu.cn (Z. Yan); xbcao@zjxu.edu.cn (X. Cao)

Contents:

Experimental Sections

Chemicals: 2, 5-thiophenedicarboxylic (H_2TDC, 98%), cobalt(II) acetate tetrahydrate ($Co(CH_3COO)_2·4H_2O$), nickel(II) acetate tetrahydrate ($Ni(CH_3COO)_2·4H_2O$), Iron(II) acetate ($Fe(CH_3COO)_2$), hydroxydiacetyl iron hydrate ($Fe(OH)(CH_3COO)_2·nH_2O$) were purchased from Shanghai Aladdin Biochemical Technology Co., Ltd. NaOH, KOH, EtOH and IrO_2 were from Sinopharm Chemical Reagent Co., Ltd. All aqueous solutions were prepared with DI water. All chemicals are analytical grade and used as received without further purification.

Synthesis of Co-MOF: H_2TDC (1 mmol), $Co(CH_3COO)_2·4H_2O$ (1 mmol), H_2O (10 mL), and EtOH (10 mL) were placed into a 50 mL polytetrafluoroethylene-lined reaction kettle. The mixture was stirred at room temperature until dissolved, subjected to 5 minutes of ultrasonic treatment, and stirred again for uniformity. The mixture was then transferred into a stainless steel autoclave and placed in a convection oven. It was heated at 100 °C for 10 hours. After cooling to room temperature, the precipitate was obtained by vacuum filtration and washed multiple times with anhydrous ethanol. Finally, the precipitate was dried in a vacuum drying oven at 60 °C for 24 hours.

Synthesis of Ni-MOF: The preparation steps of Ni-MOF are similar to Co-MOF, with the difference being that $Co(CH_3COO)_2·4H_2O$ (1 mmol) was replaced by $Ni(CH_3COO)_2·4H_2O$ (1 mmol).

Synthesis of Co_1Ni_1-MOF: H_2TDC (1 mmol), $Ni(CH_3COO)_2·4H_2O$ (0.5 mmol), $Co(CH_3COO)_2·4H_2O$ (0.5 mmol), H_2O (10 mL), and E_tOH (10 mL) were placed into a 50 mL polytetrafluoroethylene-lined reaction kettle. The mixture was stirred at room temperature until dissolved, subjected to 5 minutes of ultrasonic treatment, and stirred again for uniformity. The mixture was then transferred into a stainless steel autoclave and placed in a convection oven. It was heated at 100 °C for 10 hours. After cooling to room temperature, the precipitate was obtained by vacuum filtration and washed multiple times with anhydrous ethanol. Finally, the precipitate was dried in a vacuum drying oven at 60 °C for 24 hours.

Synthesis of $(Co_1Ni_1)_2Fe_1$(II)-MOF: H_2TDC (1 mmol), $Ni(CH_3COO)_2·4H_2O$ (0.33 mmol), $Co(CH_3COO)_2·4H_2O$ (0.33 mmol), $Fe(CH_3COO)_2$ (0.33 mmol), H_2O (10 mL), and EtOH (10 mL) were placed into a 50 mL polytetrafluoroethylene-lined reaction kettle. The mixture was stirred at room temperature until dissolved, subjected to 5 minutes of ultrasonic treatment, and stirred again for uniformity. The mixture was then transferred into a stainless steel autoclave and placed in a convection oven. It was heated at 100 °C for 10 hours. After cooling to room temperature, the precipitate was obtained by vacuum filtration and washed multiple times with anhydrous ethanol. Finally, the precipitate was dried in a vacuum drying oven at 60 °C for 24 hours.

Synthesis of $(Co_1Ni_1)_2Fe_1$(III)-MOF: The preparation steps of $(Co_1Ni_1)_2Fe_1$(III)-MOF are similar to $(Co_1Ni_1)_2Fe_1$(II)-MOF, with the difference being that $Fe(CH_3COO)_2$ (0.33 mmol) was replaced by $Fe(OH)(CH_3COO)_2·nH_2O$ (0.33 mmol).

Materials Characterization: The morphology and structure of the MOFs were analyzed by scanning electron microscopy (SEM, Hitachi S-4800) with energy dispersive spectroscopy (EDS). Infrared spectra were carried out by a THERMO NicoletNexus 470 FT-IR spectrometer. XRD-7000 was used to collect the powder X-ray diffraction (PXRD) patterns with a Cu Kα radiation source, which was produced by SHIMADZU. Thermogravimetric analysis (TGA) was conducted by the NETZSCH SAT-409PC in a nitrogen flow. The content of transition metals such as Co, Ni, and Fe was measured using X-ray photoelectron spectroscopy (XPS, THERMO ESCALAB 250Xi) and Inductively Coupled Plasma Spectrometer (ICP, Agilent ICP-OES720).

Electrochemical measurement. Electrochemical measurements were implemented in a three-electrode system with an Hg/HgO (0.1 M KOH) electrode as the reference electrode and a carbon rod as the counter electrode, and a glassy carbon (GC) electrode loaded with MOFs was used as the working electrode. All potentials are calculated by the Nernst equation (E (V vs. RHE) = E (V vs. Hg/HgO) + 0.0977 + 0.059 pH), using the reversible hydrogen electrode (RHE) as a reference. The catalyst

ink was prepared by the following method: fully ground 10 mg catalyst and 10 mg conductive carbon powder in a mortar, then take 5 mg of the above-mixed powder into a 2 mL centrifugation tube, 460 μL isopropanol and 40 μL Nafion solution were added and ultrasonication for 45 minutes. Spread 5 μL of homogeneous solution evenly on a freshly polished glassy carbon electrode and place it in an infrared drying oven for complete drying. The catalyst mass loading is approximately 0.36 mg cm^{-2}. The linear scan voltammetry (LSV) curves of obtained MOFs were recorded with an applied potential window of 0-0.8 V vs. Hg/HgO, the scan rate is 5 mV s^{-1}. The electrochemically active surface areas (ECSAs) are usually estimated from the electrochemical double-layer capacitance (C_{dl}) via collecting cyclic voltammograms (CVs).[1-3] The C_{dl} was determined from cyclic voltammograms measured in a non-Faradaic region at different scan rates in the potential range from 0 to 0.1 V versus Hg/HgO. The current differences at 0.1 V against (v= 10, 20, 30, 40, 80 and 160 mV/s) were fitted to obtain the C_{dl}: $C_{dl} = I_c/v$, where C_{dl}, I_c, and v are the double-layer capacitance (mF/cm^2) of the electroactive materials, charging current (mA/cm^2), and scan rate (mV/s). The electrochemical impedance spectroscopy (EIS) was recorded with the applied potential of 0.65 V versus RHE, and the frequency scan range was from 10^{-2} Hz to 10^5 Hz.

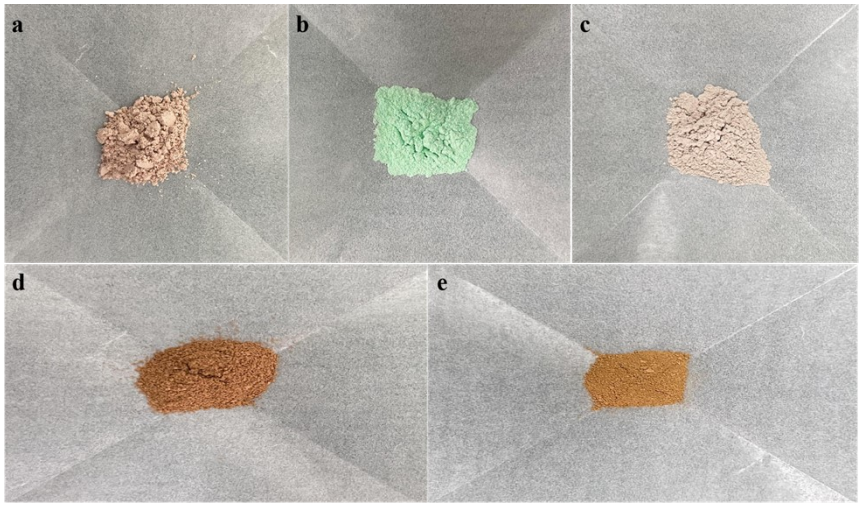

Fig. S1 Sample diagram. (a) **Co-MOF**, (b) **Ni-MOF**, (c) **Co_1Ni_1-MOF**, (d) **$(Co_1Ni_1)_2Fe_1$(II)-MOF**, (e) **$(Co_1Ni_1)_2Fe_1$(III)-MOF**.

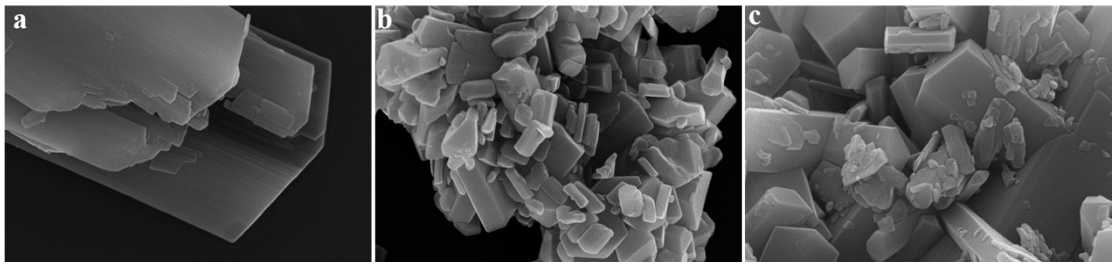

Fig. S2 SEM images. (a) **Co-MOF**, (b) **Ni-MOF**, (c) **Co_1Ni_1-MOF**.

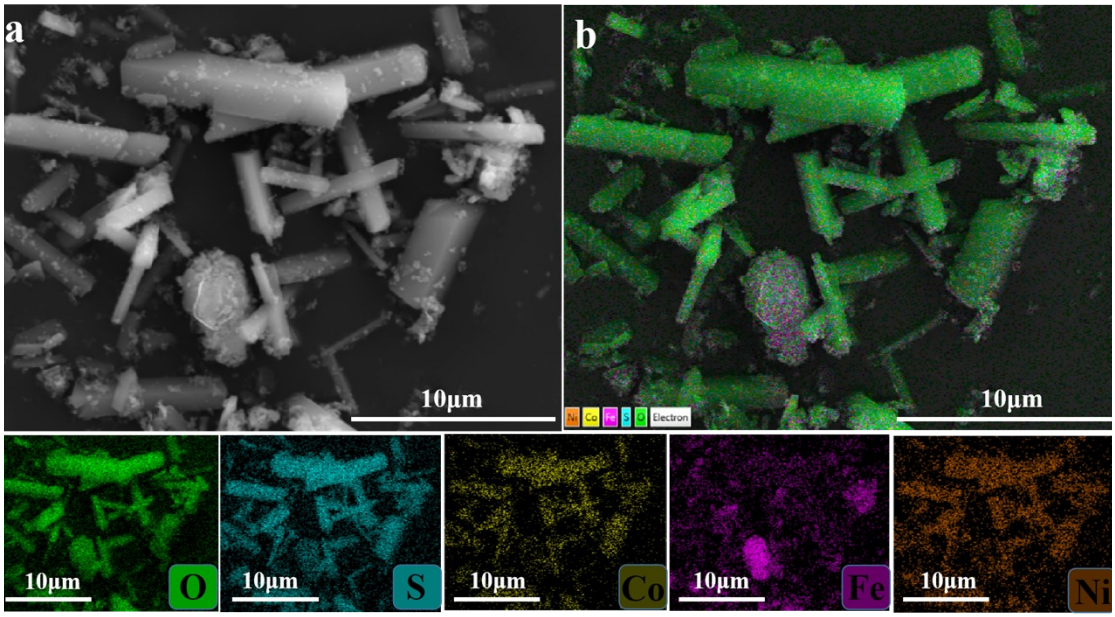

Fig. S3 (a) SEM image of **$(Co_1Ni_1)_2Fe_1$(III)-MOF**. (b) EDS layered images and elemental mapping images of **$(Co_1Ni_1)_2Fe_1$(III)-MOF**.

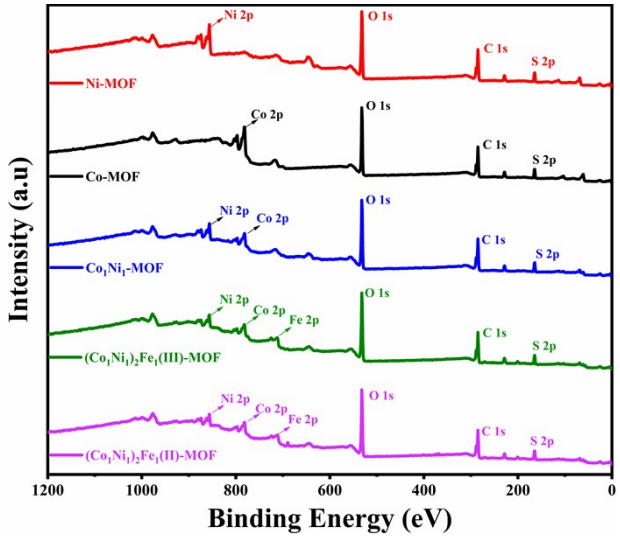

Fig. S4 Full XPS Survey spectrum of the five MOFs.

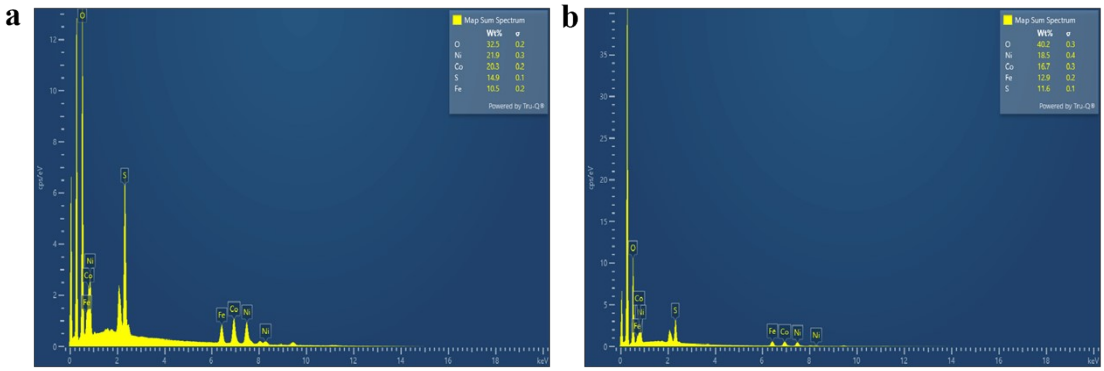

Fig. S5 EDS Elemental Analysis. (a) $(Co_1Ni_1)_2Fe_1$(II)-MOF, (b) $(Co_1Ni_1)_2Fe_1$(III)-MOF.

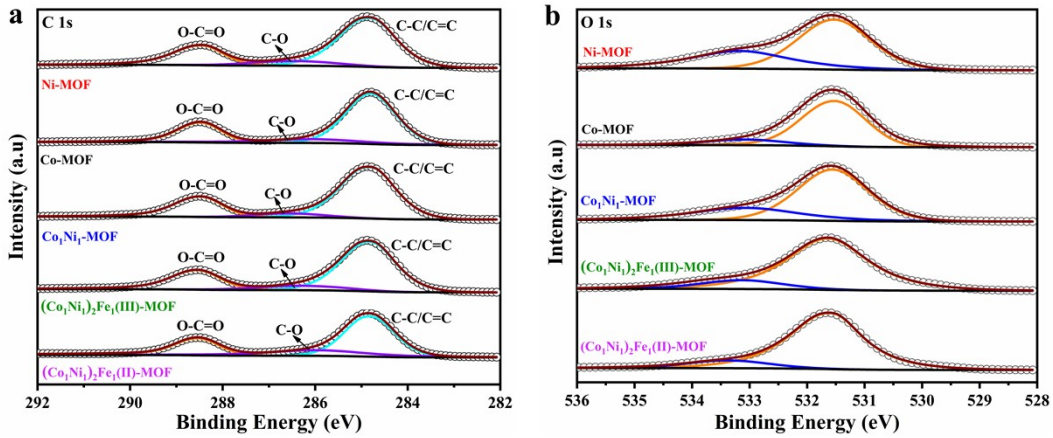

Fig. S6 High-resolution spectra of five MOFs. (a) C 1s, (b) O 1s.

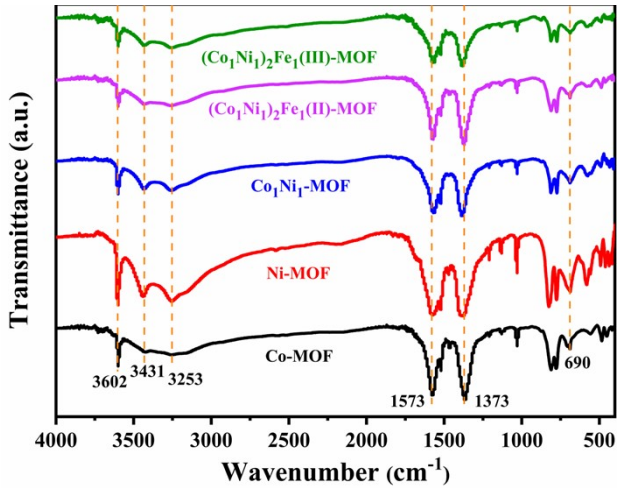

Fig. S7 FT-IR spectrum of five MOFs.

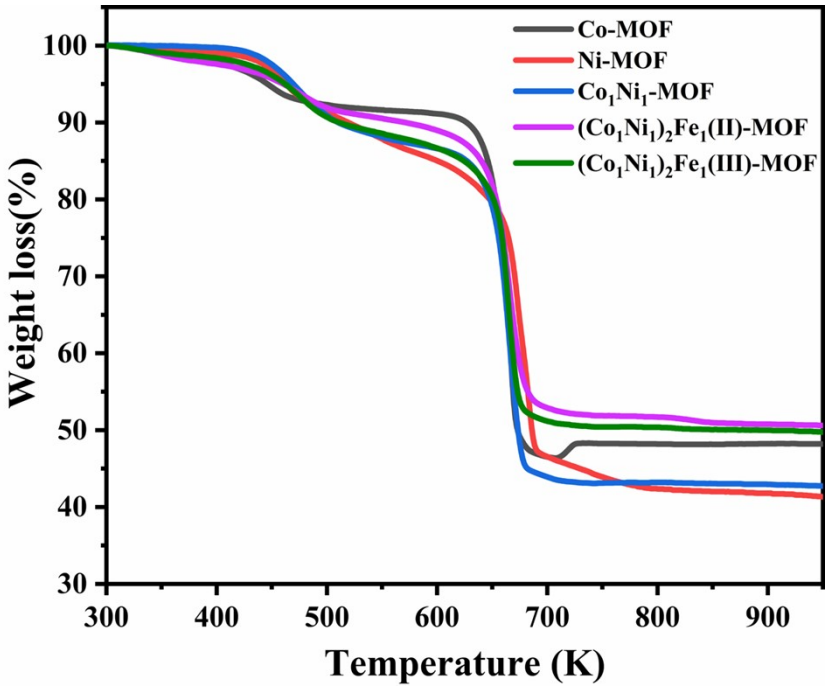

Fig. S8 TGA of five MOFs.

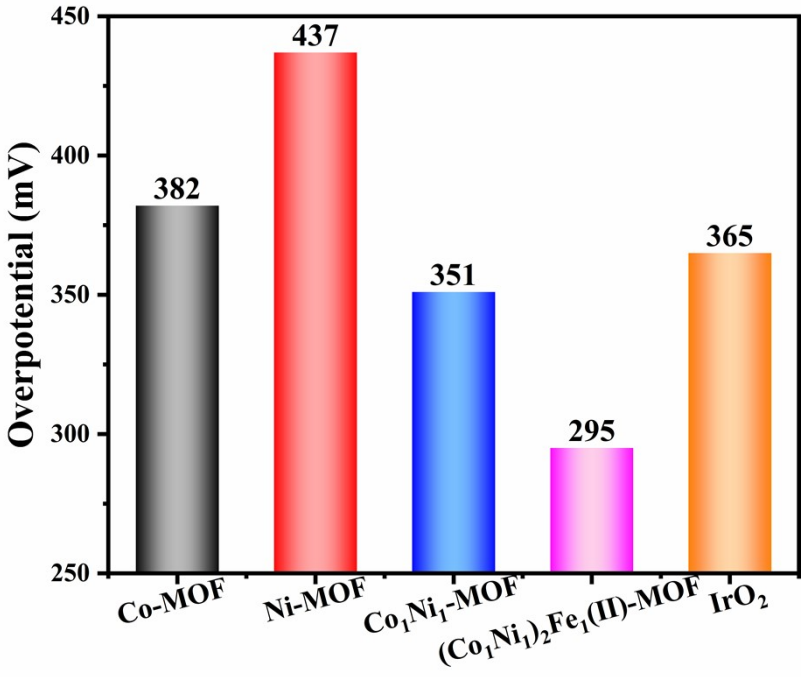

Fig. S9 Overpotential at current density of 10 mA cm^{-2}.

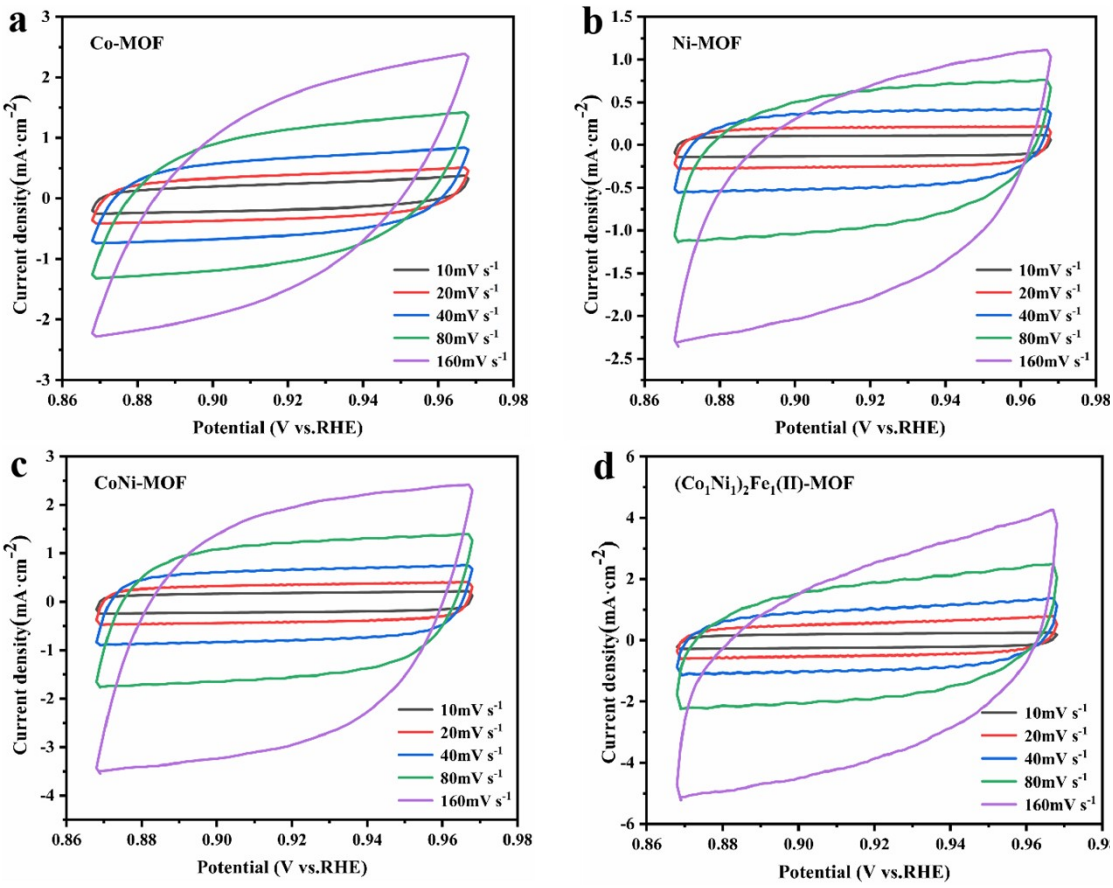

Fig. S10 CV curves. (a) **Co-MOF**, (b) **Ni-MOF**, (c) **Co_1Ni_1-MOF**, (d) **$(Co_1Ni_1)_2Fe_1$(II)-MOF**.

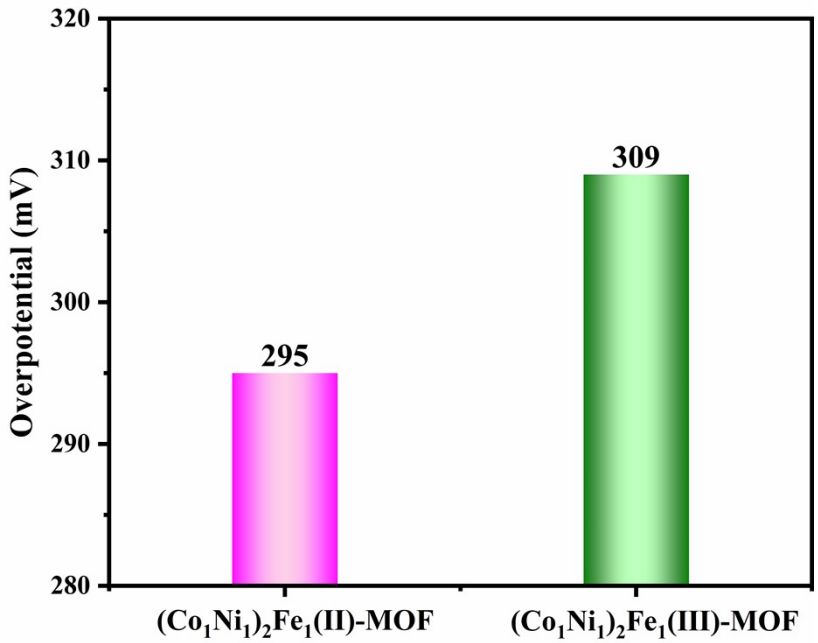

Fig. S11 Overpotentials of two different valence trimetallic doped MOFs at a current density of 10 mA cm^{-2}.

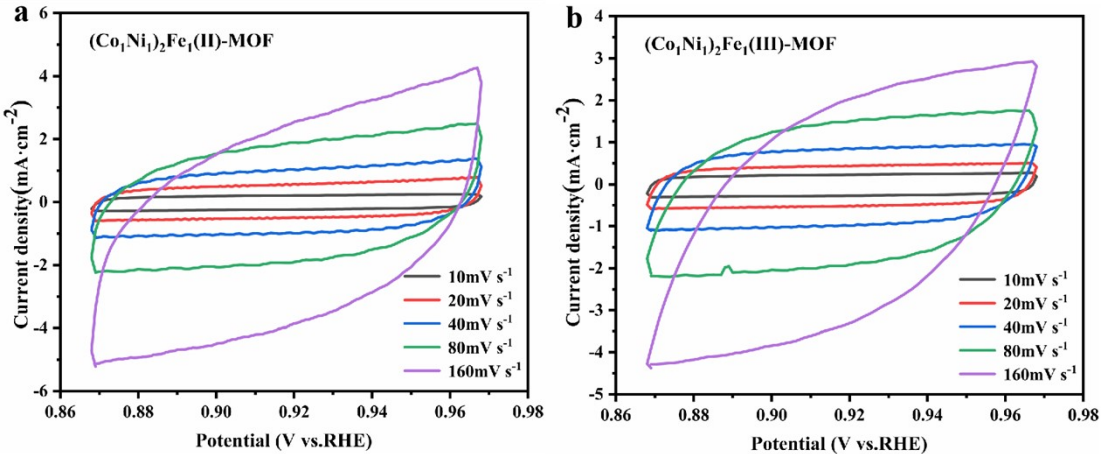

Fig. S12 CV curves of two MOFs. (a) **$(Co_1Ni_1)_2Fe_1$(II)-MOF**, (b) **$(Co_1Ni_1)_2Fe_1$(III)-MOF**.

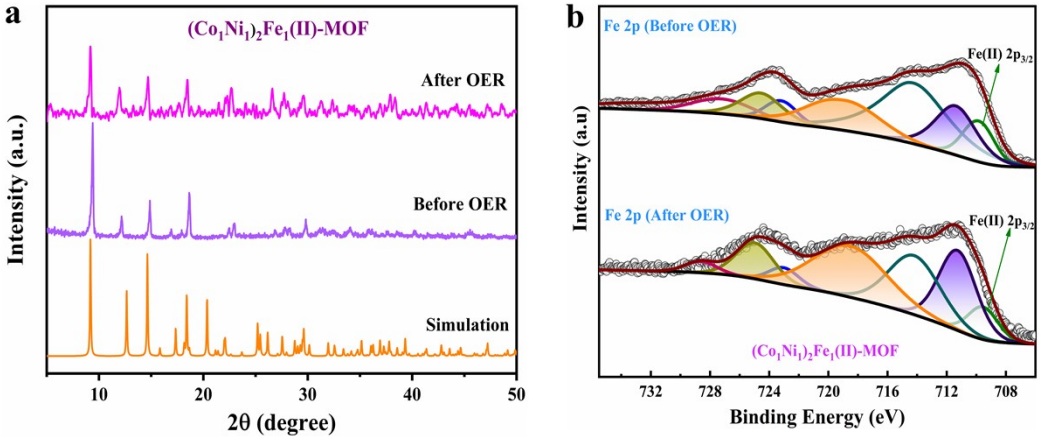

Fig. S13 Comparison of the (a) XRD patterns and (b) XPS spectra of **$(Co_1Ni_1)_2Fe_1$(II)-MOF** before and after OER reaction.

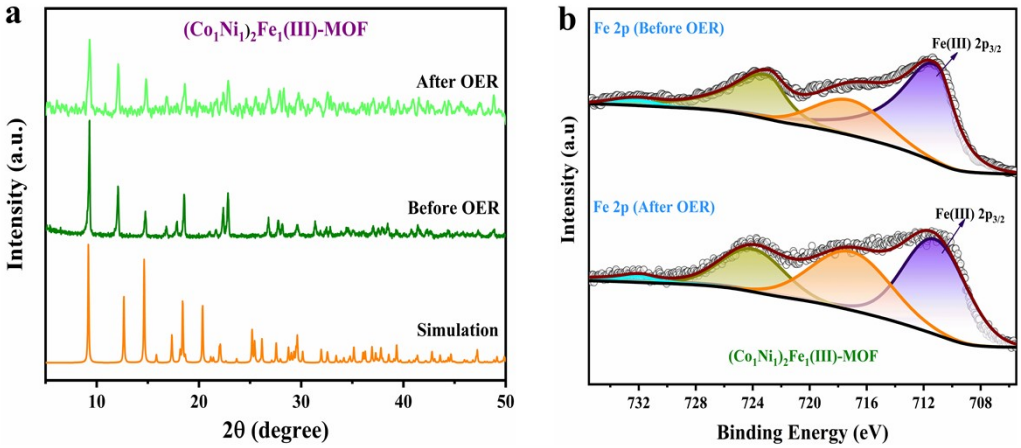

Fig. S14 Comparison of the (a) XRD patterns and (b) XPS spectra of **$(Co_1Ni_1)_2Fe_1$(III)-MOF** before and after OER reaction.

Table S1. XPS high-resolution spectrum of **$(Co_1Ni_1)_2Fe(II)$-MOF** (Co/Ni/Fe=5.15/5.10/4.83)

$(Co_1Ni_1)_2Fe_1(II)$-MOF	FWHM eV	Area (P) CPS.eV	Atomic %
Co	3.14	200608.36	5.15
Ni	2.25	197587.82	4.83
Fe	6.02	167602.53	5.10

Table S2. XPS high-resolution spectrum of **$(Co_1Ni_1)_2Fe_1(III)$-MOF** (Co/Ni/Fe=4.80/4.75/5.16).

$(Co_1Ni_1)_2Fe_1(III)$-MOF	FWHM eV	Area (P) CPS.eV	Atomic %
Co	3.74	177222.22	4.80
Ni	2.25	184413.36	4.75
Fe	4.90	160787.21	5.16

Table S3. ICP analysis for **$(Co_1Ni_1)_2Fe_1(II)$-MOF** (Co/Ni/Fe=1.983/1.973/2.050).

$(Co_1Ni_1)_2Fe_1(II)$-MOF	Sampling quality (g)	Volume (mL)	Coefficient of dilution	Instrument readings (mg/L)	Molar ratio
Co	0.0346	25	100	1.6176	1.983
Ni	0.0346	25	100	1.6025	1.973
Fe	0.0346	25	100	1.5889	2.050

Table S4. ICP analysis for **$(Co_1Ni_1)_2Fe_1(III)$-MOF** (Co/Ni/Fe=2.073/2.046/2.209).

$(Co_1Ni_1)_2Fe_1(III)$-MOF	Sampling quality (g)	Volume (mL)	Coefficient of dilution	Instrument readings (mg/L)	Molar ratio
Co	0.0376	25	100	1.8375	2.073
Ni	0.0376	25	100	1.8059	2.046
Fe	0.0376	25	100	1.8606	2.209

Table S5. Electrocatalytic OER activities of MOF-based and the state-of-the-art non-MOFcatalysts in 0.1 M alkaline electrolyte between recently reported studies and this work.

Catalyst	***Over potential @ 10 mA cm^{-2}***	***Tafel slope (mV dec^{-1})***	***Substrate***	***Ref.***
β-$Co(OH)_2$/Co-MOF	*405*	*124*	GC	*[4]*
$Ni_{0.8}Fe_{0.2}$-MOF-B	*301*	*62*	GC	*[5]*
ZIF-62-(Co)-Fe-CC	*335*	*44.3*	*CC*	*[6]*
$[Co_7(t\text{-}ca)_{14}(H_2O)_2]$	*361*	*53*	GC	*[7]*
Co-BTC-IMI	*360*	*88*	*RDE*	*[8]*
CTGU-10c2	*240*	*58*	*GC*	*[9]*
CoFe-PYZ	*300*	*44*	*GC*	*[7]*
2D CoZIF-9(III) sheets	*380*	*55*	*GC*	*[8]*
2D-Co-NS	*310*	*81*	*GC*	*[9]*
CoFe-MOF	*355*	*49.05*	*GC*	*[10]*
Fe_3-Co_2	*283*	*43*	*GC*	*[11]*
Co:Fe_3	*453*	*63*	*GC*	*[12]*
Fe_3-Fe	*460@1mA cm^{-2}*	*137*	*GC*	*[13]*
Fe_3	*482@1mA cm^{-2}*	*112*	*GC*	*[14]*
FeCo-MNS	*298*	*21.6*	*GC*	*[15]*
CoBDC	*490*	*48.8*	*GC*	*[16]*
MOF-H_2	*337(η_j=15)*	*N/A*	*GC*	*[17]*
MAF-X27-OH	*461*	*66*	*GC*	*[18]*
Co-WOC-1	*390@1mA cm^{-2}*	*128*	*GC*	*[19]*
W-625[a]	*327±7*	-	-	*[20]*
W-718[a]	*320±10*	-	-	*[20]*

W-825[a]	*322±3*	-	-	*[20]*
W-286[a]	*339±4*	-	-	*[20]*
W-316L[a]	*340±20*	-	-	*[20]*
IrO_2, 20 μg cm^{-2}	*400±10*	-	*GC*	*[20]*
IrO_2, 100 μg cm^{-2}	*354±3*	-	*GC*	*[20]*
Fe-Ni LDH	*130*	-	*e-Ni foil[b]*	*[21]*
Electrodeposited Fe–Ni film (Fe/Ni=0.67)	*280*	-	-	*[22]*
$Ni(OH)_2$	*573*	-	*RDE*	*[23]*
NiFe LDH	*348*	-	*RDE*	*[23]*
AISI 304 activated steel (Elox300)	*269*	*66*	-	*[24]*
Three-dimensional S235 steek (phosphorization)	*326*	*68.7*	-	*[25]*
IrO_2, 210 μg cm^{-2}	*330*	-	*GC*	*[26]*
$(Co_1Ni_1)_2$Fe(II)-MOF	***295***	***48.48***	***GC***	***This work***
$(Co_1Ni_1)_2$Fe(III)-MOF	***309***	***97.04***	***GC***	***This work***

References

[1] Li, F.-L.; Shao, Q.; Huang, X.-Q.; Lang, J.-P. *Angew. Chem. Int.* **2018**, 57, 1888-1892.

[2] C. McCrory, S. Jung, I. M. Ferrer, S. M. Chatman, J. C. Peters, T. F. Jaramillo, *J. Am. Chem. Soc.* **2015**, 137, 4347-4357.

[3] Chen, R.; Wang, H.-Y.; Miao, J.; Yang, H.; Liu, B.; *Nano Energy.* **2015**, 11, 333-340.

[4] Wu, J.-Q.; Zhao, Z.-H.; Hua, Y.-W.; Wu, Y.-L.; Ye, S.-Y.; Qian, J.-T.; Li, M.-L.; Zhu, L.-W.; Yan, Z.; Cao, X. *Inorg. Chem*. **2023**, *62*, 15641−15650.

[5] Zhang, H.-D.; Wu, Y.-L.; Ye, S.-Y.; Hua, Y.-W.; You, X.-X.; Yan, Z.; Li, M.-L.; Liu, D.; Meng, Y.; Cao, X. *ChemElectroChem* **2022**, *9*, e202200246.

[6] Lin, R.; Li, X.; Krajnc, A.; Li, Z.; Li, M.; Wang, W.; Zhuang, L.; Smart, S.; Zhu, Z.; Appadoo, D.; Harmer, JR.; Wang, Z.; Buzanich, AG.; Beyer, S.; Wang, L.; Mali, G.; Bennett, TD.; Chen, V.; Hou, J. *Angew. Chem., Int. Ed*. **2022**, *61*, e202112880.

[7] Kang, J.; Lee, M. J.; Oh, N. G.; Shin, J.; Kwon, S. J.; Chun, H.; Kim, S. J; Yun, H.; Jo, H.; Ok, K. M.; Do, J. *Chem. Mater*. **2021**, *33*, 2804–2813.

[8] Wang, H.; Zhang, X.; Yin, F.; Chu, W.; Chen, B. *J Mater. Chem. A*, **2020**, *8*, 22111–22123

[9] Zhou, W.; Huang, D.; Wu, Y.; Zhao, J.; Wu, T.; Zhang, J.; Li, D.; Sun, C.; Feng, P.; Bu, X. *Angew. Chem., Int. Ed.* **2019**, *58*, 4227-4231.

[10] Gao, J.; Cong, J.; Wu, Y.; Sun, L.; Yao, J.; Chen, B. *ACS Appl. Energy Mater.* **2018**, *1*, 5140-5144.

[11] Jayaramulu, K.; Masa, J.; Morales, D. M.; Tomanec, O.; Ranc, V.; Petr, M.; Wilde, P.; Chen, Y.-T.; Zboril, R.; Schuhmann, W.; Fischer, R. A. *Adv. Sci.* **2018**, *5*, 1801029.

[12] Huang, J.; Li, Y.; Huang, R.-K.; He, C.-T.; Gong, L.; Hu, Q.; Wang, L.; Xu, Y.-T.; Tian, X.-Y.; Liu, S.-Y.; Ye, Z.-M.; Wang, F.; Zhou, D.-D.; Zhang, W.-X.; Zhang, J.-P. *Angew. Chem., Int. Ed.* **2018**, *57*, 4632-4636.

[13] Yang, C.; Cai, W.-J.; Yu, B.-B.; Qiu, H.; Li, M.-L.; Zhu, L.-W.; Yan, Z.; Hou, L.; Wang, Y.-Y. *Catal. Sci. Technol*. **2020**, *10*, 3897-3903.

[14] Shen, J.-Q.; Liao, P.-Q.; Zhou, D.-D.; He, C.-T.; Wu, J.-X.; Zhang, W.-X.; Zhang, J.-P.; Chen, X.-M. *J. Am. Chem. Soc*. **2017**, *139*, 1778-1781.

[15] Zhan, G.; Fan, L.; Zhao, F.; Huang, Z.; Chen, B.; Yang, X.; Zhou, S.-f. *Adv. Funct. Mater.* **2019**, *29*, 1806720.

[16] Zhao, L.; Dong, B.; Li, S.; Zhou, L.; Lai, L.; Wang, Z.; Zhao, S.; Han, M.; Gao, K.; Lu, M.; Xie, X.; Chen, B.; Liu, Z.; Wang, X.; Zhang, H.; Li, H.; Liu, J.; Zhang, H.; Huang, X.; Huang, W. *ACS Nano* **2017**, *11*, 5800-5807.

[17] Jiang, Z.; Ge, L.; Zhuang, L.; Li, M.; Wang, Z.; Zhu, Z. *ACS Appl. Mater. Interfaces* **2019**, *11*, 44300-44307.

[18] Lu, X.-F.; Liao, P.-Q.; Wang, J.-W.; Wu, J.-X.; Chen, X.-W.; He, C.-T.; Zhang, J.-P.; Li G.-R.; Chen, X.-M. *J. Am. Chem. Soc*. **2016**, 138, 8336–8339.

[19] Manna, P.; Debgupta, J.; Bose, S.; Das, S. K. *Angew. Chem., Int. Ed*. **2016**, 55, 2425-2430.

[20] Magnier, L.; Cossard, G.; Martin, V.; Pascal, C.; Roche, V.; Sibert, E.; Shchedrina, I.; Bousquet, R.; Parry, V.; Chatenet, M. *Nat. Mater.* **2024**, 23, 252-261.

[21] Xiang, Q.; Li, F.; Chen, W.-L.; Ma, Y.-L.; Wu, Y.; Gu, X.; Qin, Y.; Tao, P.; Song, C.-Y.; Shang, W.; Zhu, H.; Deng, T.; Wu, J.-B. *ACS Energy Lett.* **2018**, 3, 10, 2357-2365.

[22] Louie, M. W.; Bell, A. T. *J. Am. Chem. Soc.* **2013**, 135, 12329-12337.

[23] Dionigi, F.; Zeng, Z.; Sinev, I.; Merzdort, T.; Deshpande, S.; Lopez, M. B.; Kunze, S.; Zegkinoglou, I.; Sarodnik, H.; Fan, D.-X.; Bergmann, A.; Drnec, J.; Araujo, J. F.; Gliech, M.; Teschner, D.; Zhu, J.; Li, W.-X.; Greeley, J.; Cuenya, B. R.; Strasser, P. *Nat Commun.* **2020,** 11, 2522.

[24] Schäfer, H.; Sadaf, S.; Walder, L.; Kuepper, K.; Dingklage, S.; Wollschläger, J.; Schneider, L.; Steinhart, M.; Hardege, J.; Daum, D. *Energy Environ. Sci.* **2015**, 8, 2685-2697.

[25] Han, W.-J.; Kuepper, K.; Hou, P.-L.; Akram, W.; Eickmeier, H.; Hardege, J.; Steinhart, M.; Schäfer, H. *Chem. Sus. Chem.* **2018**, 11, 3661-3671.

[26] Liu, L.-X.; Liu, W.; Ko, M.; Park, M.; Kilm, M. G.; Oh, P.; Chase, S.; Park, S.; Casimir, A.; Wu, G.; Cho, *J. Adv. Funct. Mater.* **2015**, 25, 5799-5808.